

GRAPH AND HEURISTIC BASED TOPOLOGY OPTIMIZATION OF CRASHWORTHINESS COMPOSITE PROFILE STRUCTURES MANUFACTURED BY VACUUM INFUSION AND GLUING

DOMINIK SCHNEIDER¹, SIMON LINK¹, AXEL SCHUMACHER¹ AND CHRISTOPHER ORTMANN²

¹ University of Wuppertal, Chair for Optimization of Mechanical Structures
Gaussstraße 20, 42119 Wuppertal, Germany
e-mail: dschneider@uni-wuppertal.de; simon.link@uni-wuppertal.de;
schumacher@uni-wuppertal.de website: <https://www.oms.uni-wuppertal.de/>

² Volkswagen Aktiengesellschaft
Letterbox 1777, 38436 Wolfsburg, Germany
e-mail: christopher.ortmann@volkswagen.de website: <http://www.volkswagen-ag.de/>

Key words: topology optimization, crashworthiness, heuristic, graph theory, composite profile, gluing.

Abstract. *Composite structures enable lightweight solutions, which are required by the transportation industry to fulfil their weight targets. Many of those structures have high requirements regarding passive safety and manufacturing. Yet finding suitable designs for crashworthiness applications proves to be difficult because of material nonlinearities, contact, large displacements and in case of composite materials anisotropy, brittle failure and crushing. The Graph and Heuristic Based Topology Optimization (GHT)^[1] has already been utilized for the optimization of metal extrusion profiles under lateral crash loads. In order to enable the use of composite materials, the graph syntax, which is used to represent the geometry, is modified, so that it can carry information regarding fiber orientations and thicknesses of the layers. During the optimization, heuristics based on expert knowledge regarding crash applications evaluate the simulation data and propose new competing layouts with modified topologies. These designs are then evaluated with a single or multiple crash simulations in inner optimization loops. During the whole optimization process various manufacturing constraints prevent the occurrence of non-manufacturable designs. This paper illustrates, how the GHT can be extended for the optimization of crashworthiness composite profile structures under lateral loads. An extension of the graph syntax allows splitted structures which are glued together at flanges. New heuristics detect element failure and try to sustain the structural integrity. An Optimization of a test specimen laterally impacted by a drop weight is carried out where the maximum contact force is minimized while restricting the maximum intrusion. Two improved designs and the initial design are manufactured and tested in a drop tower. The test results are presented and compared with the simulations.*

1 INTRODUCTION

Composite materials enable lightweight structures because of their low density and high specific strength. In addition they show very good energy absorption capabilities if failing through stable crushing. They offer a great variety of design freedoms, like the type of matrix and fiber, the orientation and volume fraction of the fibers or the manufacturing process.

The large number of design freedoms and manufacturing constraints complicate the component development for crash applications. Popular commercially available topology optimization methods for linear static problems^[2,3] cannot be utilized in the process because of material nonlinearities, contact, large displacements and the explicit finite element method. Other methods^[4] try to overcome these issues. The Graph and Heuristic Based Topology Optimization (GHT)^[1] can be utilized to optimize the topology of structures with a constant cross section like extrusion profiles or rib layouts^[5]. The cross-section is described by a mathematical graph which enables algorithmic manipulations of the geometry while allowing to check manufacturing constraints. Heuristics that are based on expert knowledge regarding crash applications are used in an outer optimization loop to suggest new designs. They insert or remove walls from designs of the previous iteration after analysing their simulation results like nodal displacements, velocities, energy densities and element deletion. Inner optimization loops evaluate all new topologies by calling the commercial optimizer LS-OPT that changes e.g. the thicknesses to reach the given optimization objective while meeting the constraints. If desired a shape and sizing optimization of the best design can be carried out at the end of the optimization to try to reach further improvements.

To extend the field of application towards composite structures with constant cross-section, some adjustments are necessary, that are described in this paper. An optimization of a test specimen is carried out to demonstrate the procedure. The structure is built up by several parts with flanges that are glued together. Two improved designs as well as the initial design are manufactured by vacuum infusion and gluing to test the structures in physical experiments. Splitting the structure in several parts avoids the need to use pultrusion as the manufacturing process, which would have led to expensive tool costs for these small quantities.

2 ADAPTIONS FOR COMPOSITE STRUCTURES WITH FLANGES

Before using composite structures in an optimization, some adaptations in the GHT process are necessary. At first new information regarding the composite layup and the flanges have to be saved in the graph and taken into account while creating the input decks for the finite element simulations. In addition the material failure has to be considered. Besides new heuristics that are needed to address the material failure, the existing heuristics have to be modified to stop analyzing the finite element results after failure occurs in the observed area, since torn apart pieces flying through the space would lead to false interpretations of the deformation behavior. Furthermore the existing manufacturing constraints like limiting the minimum distance between two walls are extended by a new constraint that forbids to attach a new wall to a location with an already existing flange.

2.1 Graph syntax

The graph contains all the relevant information to describe the geometry of a structure with a constant cross section. As shown in Figure 1 each wall consists of different vertices connected by edges. The LINK-Vertices define the location of the walls with Cartesian coordinates. The BEAMG-Vertices save the thickness of each wall as well as its curvature and, in case of prescribed flange connections on outer walls, additional parameters like the overlapping length and the flange position. The BEAM1- and BEAM2-Vertices define the layer angles and layer fractions of a symmetrical composite layup or stay empty in case of applications with metal. Finally the PARAM-Vertex stores global parameters that describe the whole structure like the extrusion length and the density of the material, to allow internal mass calculations. In case of other applications like finding rib layouts^[5] the vertices can contain additional information like rib heights.

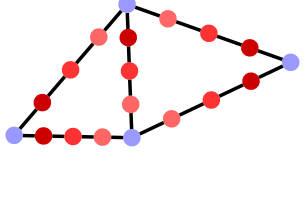
Graph Element	Contained information	
● BEAMG-Vertex	thickness, curvature, flange information	
● BEAM1-Vertex	composite layer angles	
● BEAM2-Vertex	composite layer fractions	
● LINK-Vertex	coordinates	
— EDGE	connected vertices	
○ PARAM-Vertex	e.g. extrusion length and density	

Figure 1: List of graph elements with their contained information, right: an exemplary graph

2.2 Flanges

There are two types of flanges currently implemented in the procedure. A custom flange connection can be defined on an outer wall by specifying the needed information in the BEAMG-Vertex. As displayed in Figure 2 the flange length, the flange position and the flange side can be stated. The overlapping length and the position are entered as a value between 0 and 1 with regard to the wall length. A position of 0 indicates that the flanges are located at the start of the wall and 1 respectively at the end, factoring in the edge direction. The side parameter controls on which side in edge direction the flange connection is established.

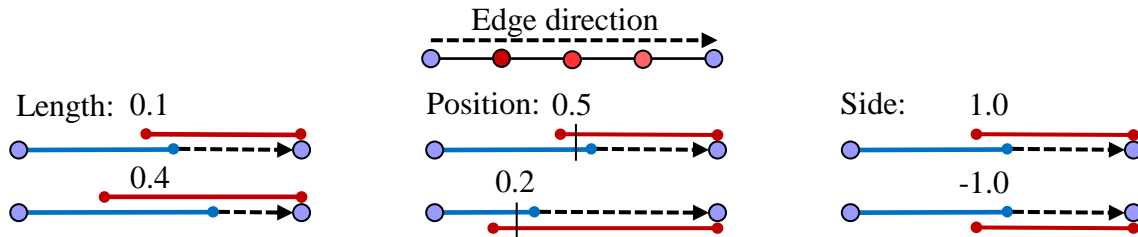


Figure 2: flange parameters, left: flange length, middle: flange position, right: side of the flange

Inner walls can automatically connect to the rest of the structure as new parts with flanges on both sides, so that each wall can be manufactured separately without undercuts. When inner walls share the same LINK-Vertex they connect to the other walls by creating a flange parallel to the next wall in clockwise direction, as displayed in Figure 3a. In case that two inner walls are connected nearly straight they are realised as a single part (Figure 3b).

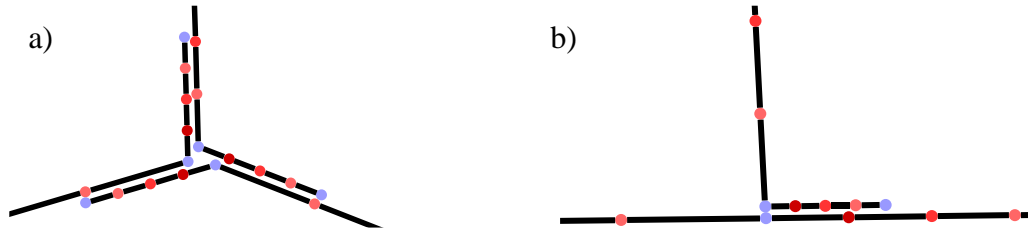


Figure 3: a) clockwise orientation of flanges of inner walls, b) no flanges created between straight connected inner walls

During the automatic creation of a finite element model, tied contacts are created between the flanges and the corresponding walls with a material defined by the user to represent the adhesive. Figure 4a shows an exemplary graph that is internally split into a converted graph (Figure 4b) with the presented rules to outline the flange connections. It is then extruded and meshed (Figure 4c) by GRAMB (Graph based Mechanics Builder), that was developed to create the input decks. As displayed, the composite layups are currently modeled with single layer elements, that contain the ply information in the material card (ESI VPS) or in the *PART_COMPOSITE definition (LS-DYNA), depending on the solver to be used. This approach saves computation time but is not capable of capturing delamination.

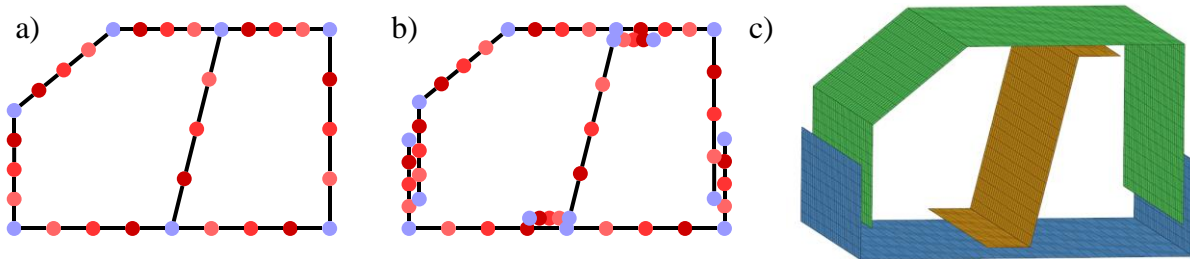


Figure 4: a) original graph, b) converted graph with flanges, c) extruded mesh

2.3 Heuristic Support Collapsing Walls

In addition to the existing heuristics^[1], the heuristic Support Collapsing Walls (SCW) is introduced to address a possible loss of the structural integrity through material failure. If detecting sudden and extensive failure, the wall with the highest failure index f is supported perpendicularly at the position of the most severe damage as displayed in Figure 5, where a cylinder impacts a structure that experiences material failure in the impact area. The failure index is calculated for each wall in each load case by formula (1).

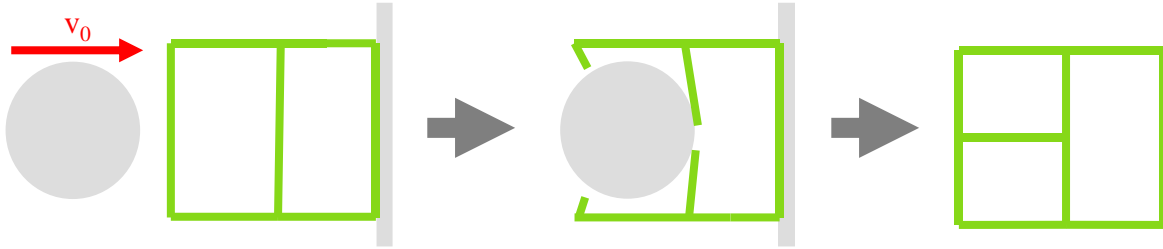


Figure 5: Principle of the heuristic Support Collapsing Walls

$$f = \max_{t_1, t_2} \left[\frac{n(t_1, t_2)}{0.9 \cdot \frac{(t_2 - t_1)}{\Delta t_{ref}} + 0.1} \right] \quad (1)$$

Here the number of elements deleted between the time t_1 and t_2 is divided by the fraction of this duration in relation to the period Δt_{ref} between the first and last occurrence of element deletion of the whole structure during the simulation. This allows to put more emphasis on strong failure in a short amount of time in contrast to less failure occurring during a longer period. To find the interval that delivers the highest failure index, t_1 and t_2 are varied in a heuristic approach to identify the maximum failure index for each wall. The heuristic then tries to support the wall with the highest failure index of all load cases perpendicular at the middle point of the deleted elements of the corresponding wall. If this fails the heuristic continues to support the wall with the next highest failure index.

2.4 Optimization variables

To evaluate the heuristic proposal, inner optimization loops can be carried out where the thicknesses of the structure are modified to improve the optimization goal. If working with composites an option is added to vary the global laminate direction that turns the complete layup of the composite. When running the final size and shape optimization, not only the thickness, the curvature and the shape can be optimized, but also the layer directions and/or the layer fractions of the layup of the whole structure. Changing the layer angles and fractions of each individual wall is not intended since it would lead to a large number of design variables that would increase the optimization time enormous and could not be handled efficiently by the optimization algorithms.

3 OPTIMIZATION OF A TEST SPECIMEN

With the new adaptations to the GHT, an optimization is carried out, that deals with a composite profile being laterally impacted by a semi-cylindrical weight in a drop tower. Since three different designs of the optimization will be manufactured and tested, the optimization problem and the simulation model are chosen to represent the test setup.

3.1 Simulation model and test setup

The simulation model is displayed on the left side of Figure 6. The rigid steel drop weight with a mass of 50 kg is guided along the Z-axis and moves with an initial velocity of 3 m/s against the Z-direction. The lower part of the drop weight has a semi-cylindrical shape with a diameter of 80 mm. The profile rests on a rigid steel plate, whose contact force with the profile is tracked during the simulation. For all contacts a friction of 0.2 is defined. The simulation is terminated by a sensor short after the drop weight starts to move back after the maximum intrusion. The model represents the test setup, visible on the right side of Figure 6. It only differs by the buffer elements on the sides that start to stop the drop weight roughly 27 mm before hitting the ground to avoid damaging the force sensor and the underlying structure in case the profile cannot stop the drop weight. Bidirectional $\pm 45^\circ$ -layers with 300 or 400 g/m² made of TENAX STS40 24K carbon fibers are used to create one of the following symmetric stacking sequences with the corresponding thicknesses assuming a fiber volume content of 48%:

- $[90^\circ, 0^\circ, 90^\circ, 0^\circ, 45^\circ, -45^\circ, 45^\circ, -45^\circ]_s \rightarrow 2.8 \text{ mm with } 300\text{g/m}^2$
- $[90^\circ, 0^\circ, 45^\circ, -45^\circ]_s \rightarrow 1.87 \text{ mm with } 400\text{g/m}^2$
- $[90^\circ, 0^\circ, 45^\circ, -45^\circ]_s \rightarrow 1.4 \text{ mm with } 300\text{g/m}^2$

The material cards for the tight contact and the composite are chosen from a set of existing cards of similar materials since no testing can be conducted to fit new material cards. Hence differences between the simulation model and the experiments are to be expected. The simulations are carried out with the commercial solver Pam-Crash.

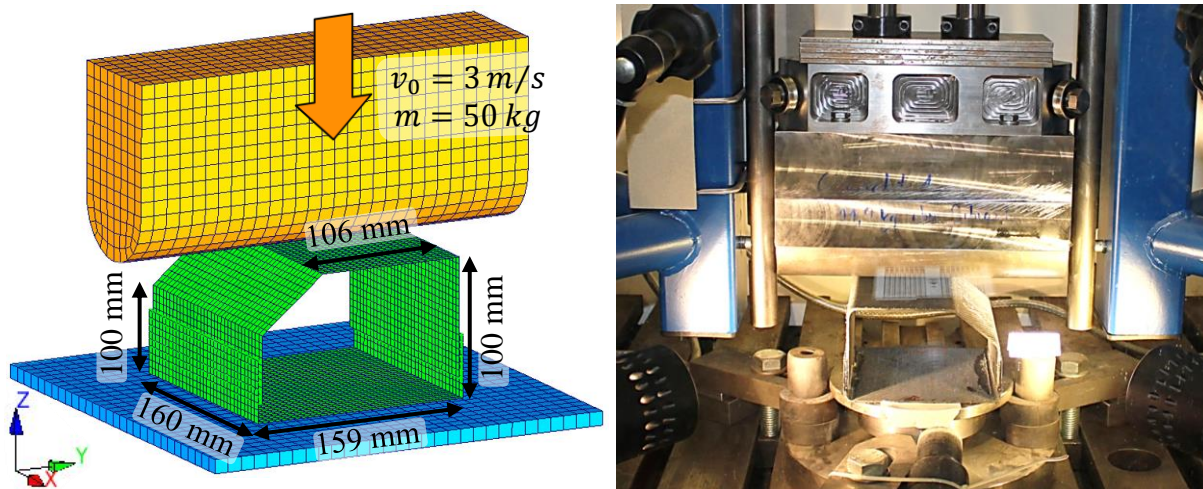


Figure 6: Simulation model (left) and corresponding test setup (right)

3.2 Optimization problem

As displayed in Table 1 the objective of the optimization is to minimize the maximum occurring force between the ground and the profile, filtered with a SAE-1000Hz-filter. The intrusion of the drop weight is restricted to 60 mm, to leave some deformation room in case the

drop weight is stopped later than predicted during the tests. During the heuristic evaluation the uniform thickness of the walls can be modified. In addition to that the shape can be varied in the final size and shape optimization. It should be mentioned that the restriction to forbid inner walls from ending at flanges of outer walls had not been implemented at the time of the optimization. All other manufacturing constraints are active and are listed in Table 1. The constraints are chosen quite restrictive to guarantee easy to manufacture structures, especially increasing the number of chambers would cause a much higher number of parts to be manufactured and glued together. During the inner optimization loops sequential domain reduction is applied combined with a genetic algorithm that is used for the optimization on the metamodel.

Table 1: Optimization problem

Objective	Minimize the maximum filtered contact force with the ground F_{max}
Constraints	Intrusion of drop weight (Z-direction) $d_z \leq 60$ mm
Design variables	Uniform thickness of the walls t Shape variables (only in final size and shape optimization)
Manufacturing constraints	Connection angle between two walls $> 60^\circ$ Wall distance > 20 mm Wall thickness > 1.4 mm and < 2.8 mm Size ratio between the largest and smallest chamber < 20 Number of chambers ≤ 3

3.3 Optimization results

The optimization starts with an empty profile without inner structures. During the Optimization in 3 Iterations 26 further designs are created and evaluated, causing about 1000 crash simulations for the heuristic evaluation and additional 1000 crash simulations for the final size and shape optimization of the so far best result. Three designs from that optimization, the initial design and the two best designs of the optimization, are chosen to be manufactured and tested. The graph and the results are displayed in Figure 7 and Table 2.

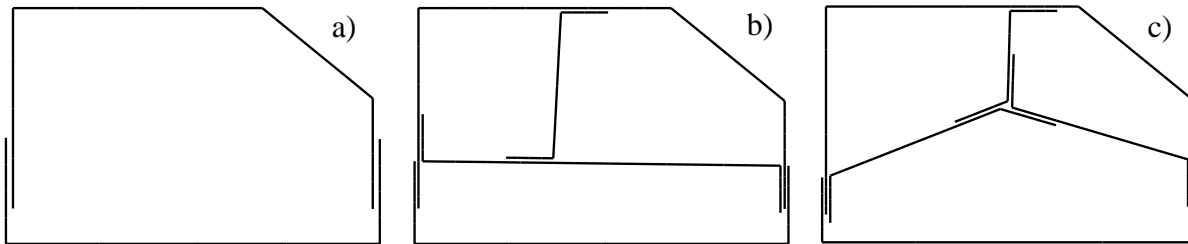


Figure 7: graphs (without vertices) of a) start design, b) option 1 and c) option 2

Table 2: Results of the selected designs from the optimization

Original Design	F_{max} [kN]	d_z [mm]	mass [kg]	t [mm]	Layup
Start	11.0	48.3	0.336	2.52	[90°,0°,90°,0°,45°,-45°,45°,-45°]s
Option 1	6.52	55.5	0.297	1.49	[90°,0°,90°,0°,45°,-45°,45°,-45°]s
Option 2	7.44	57.9	0.332	1.61	[90°,0°,90°,0°,45°,-45°,45°,-45°]s

The initial design only uses 80% of the allowed intrusion since a further reduction of the thickness would lead to a complete failure of the structure without stopping the mass. The new topologies meet the requirements to only consist of 3 chambers and are able to reduce the maximum force by 41% respectively 32%.

Since the optimization with continuous thicknesses delivers designs, that cannot be manufactured, the layups of the 3 designs are matched with the best fitting available stacking sequence for the inner and outer walls and new simulations are carried out (results in Table 3).

Table 3: Results of the adjusted designs

Adjusted Design	F_{max} [kN]	d_z [mm]	mass [kg]	t_{inner} [mm]	t_{outer} [mm]	Layup
Start S	15.3	26.0	0.372	-	2.8	[90°,0°,90°,0°,45°,-45°,45°,-45°]s
Option1 O1	7.72	55.3	0.313	1.87	1.4	[90°,0°,45°,-45°]s
Option2 O2	8.14	57.9	0.326	1.87	1.4	[90°,0°,45°,-45°]s

4 COMPARISON OF SIMULATION AND EXPERIMENT

For each adjusted design five test examples are manufactured by vacuum infusion and later glued together to create the structures displayed in Figure 8. Three of each structure are then tested in a drop tower and the results are compared with the simulations. The tests should deliver more knowledge about crash applications with composite profiles and point out necessary adjustments of the flange creation and new proposals for heuristics. Since not all structures are able to stop the drop weight before it hits the puffer elements, one of each structure is tested with a lower velocity of 2.45 m/s.

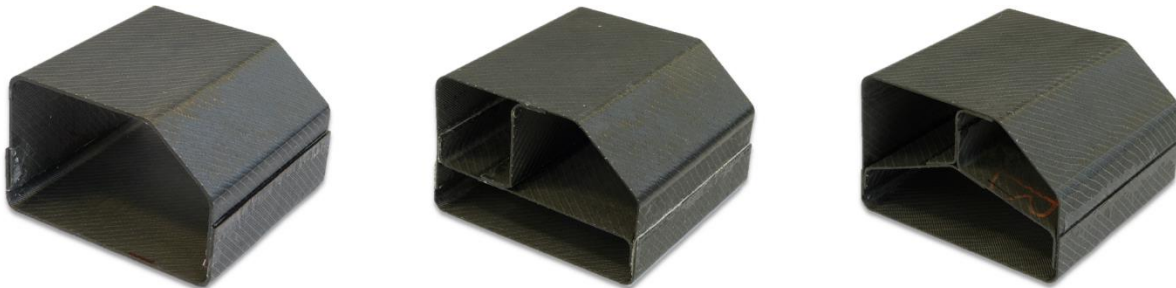


Figure 8: The manufactured profiles

4.1 Starting design S

As displayed in Figure 9 and Figure 10 all tests of the start design S as well as the simulation are able to stop the drop weight although the maximum intrusion varies between 20 mm for experiment S-3 with the lower velocity and 40 mm for S-1. The simulation S-Sim delivers the highest peak force of 15.3 kN whereas the tests show more smooth force curves that reach between 9.6 and 12.8 kN. The general deformation behavior from the tests matches the simulation quite well, although the simulation develops a crack in the upper left corner. All flange connections remain undamaged during the tests and the simulation.

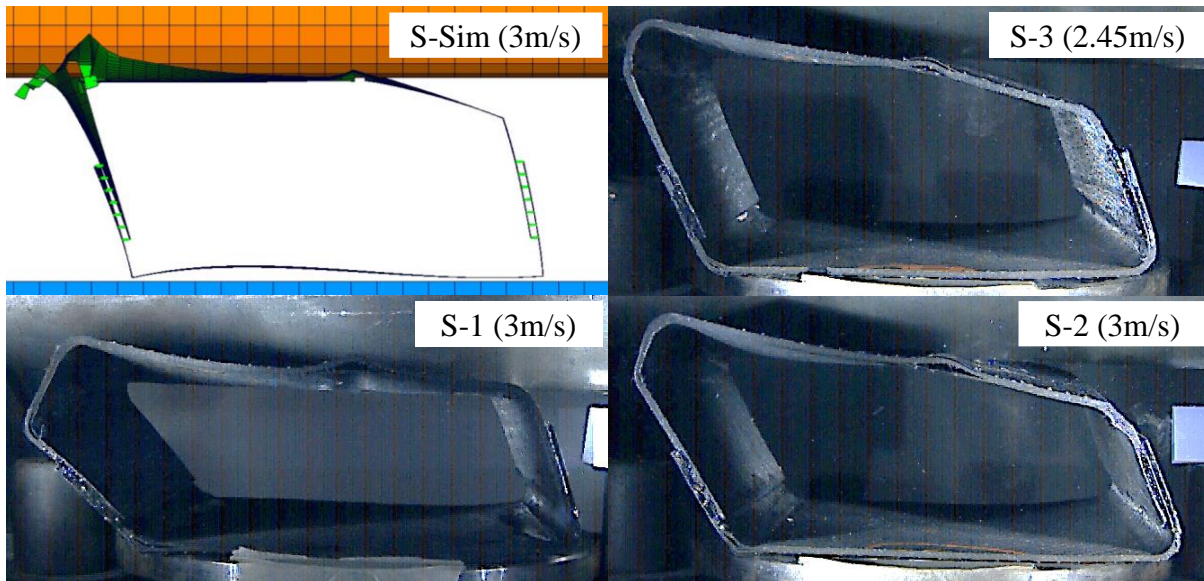


Figure 9: Deformations of the start designs S

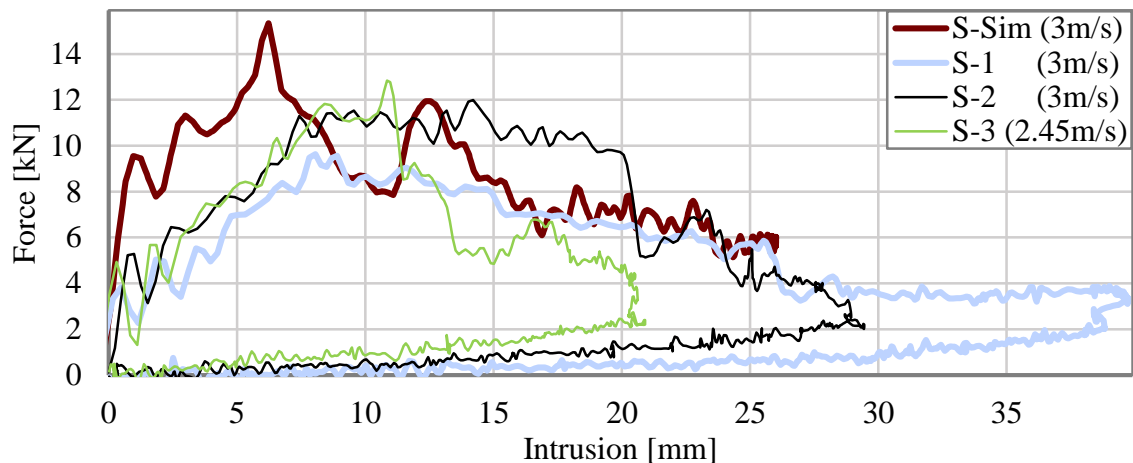


Figure 10: Force curves of the start designs S

4.2 Optimization result O1

Figure 11 reveals more differences between the deformation behavior of the simulation and the tests. While the upper wall is torn apart in the simulation and some more areas experience damage, the tests reveal failing flange connections that in case of O1-2 even lead to the drop weight crushing the structure and only getting stopped by the puffer elements. During the deformation of O1-1 and O1-3 the flange on the left side fails but the perpendicular middle wall gets in contact with the ground and stays stable so that it increases the resistance against the drop weight and stops it. The force curves in Figure 12 also reveal the differing deformation behaviors. The maximum forces range between 5.3 kN for O1-3 and 10.4 kN for O1-1, although O1-2 could have also experienced a peak at the end if the energy of the drop weight had not been absorbed by the puffers, that were placed next to the force measuring plate. The intrusions vary between 52.1 mm (O1-3) and more than 81.8 mm (O1-2).

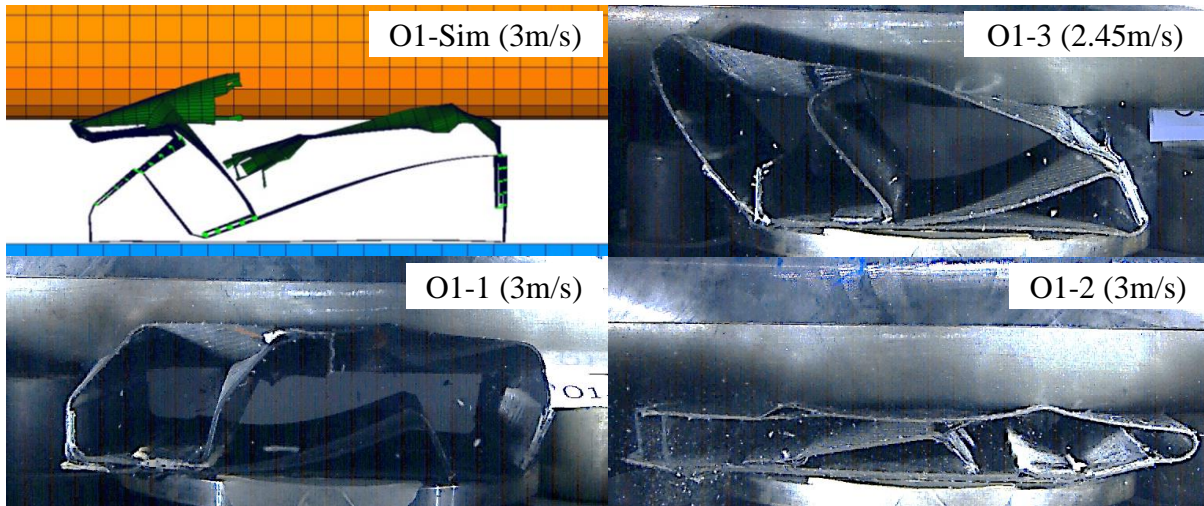


Figure 11: Deformations of the options 1 (O1)

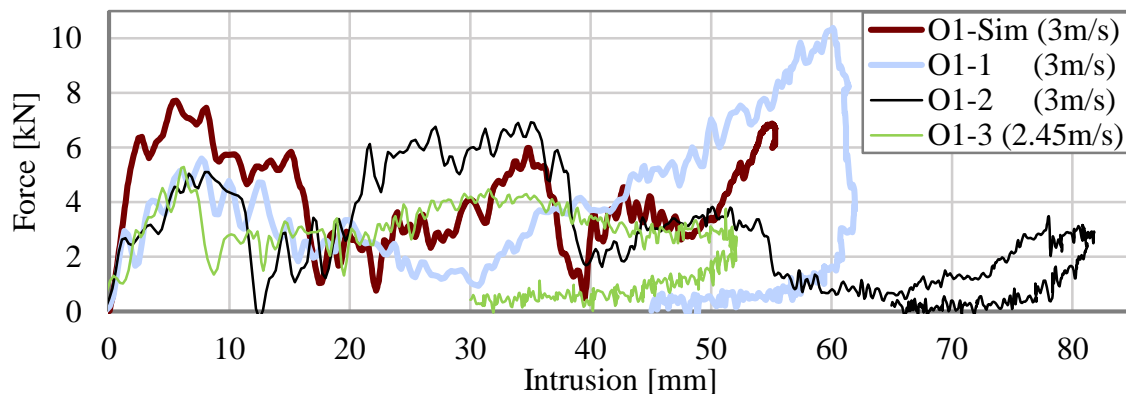


Figure 12: Force curves of the options 1 (O1)

4.3 Optimization result O2

The results for O2 are shown in Figure 13. The results of O2-1 do not exist since the recording failed. Nevertheless in comparison to O1 the same difference of tearing and failing walls in the simulation versus detached flanges in the tests occurs. During the tests the perpendicular walls get in contact with the ground and resist against the drop weight and cause a higher force level towards the end of the simulation (Figure 14). The forces vary between 5.9 kN for O2-3 and 8.1 kN for O2-Sim and the intrusions between 57.9 mm for O2-Sim and 75.4 mm for O2-2, which comes slightly in contact with the puffer elements. Both tests exceed the allowed intrusion of 60 mm.

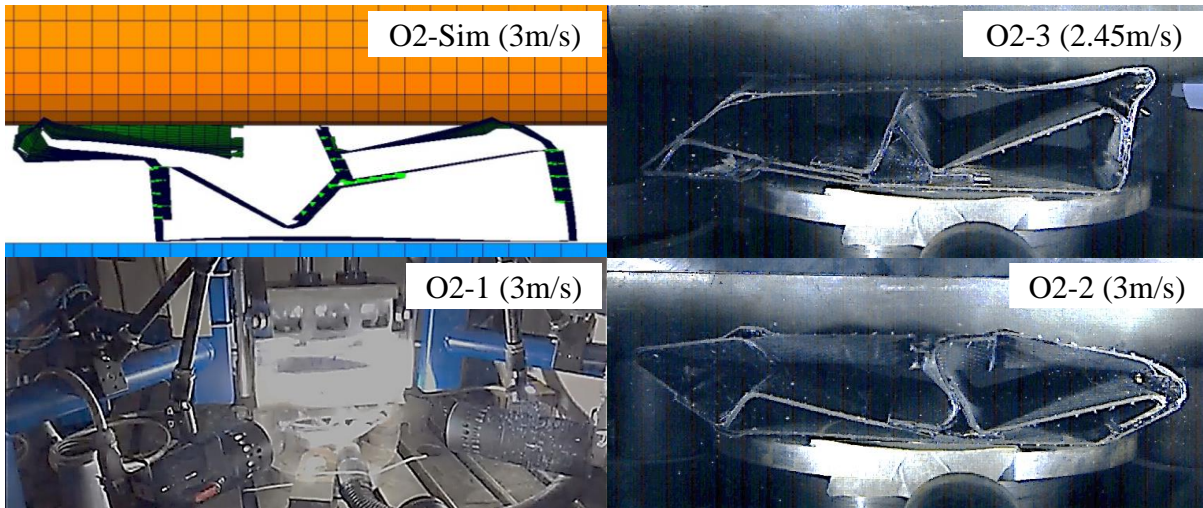


Figure 13: Deformations of the options 2 (O2)

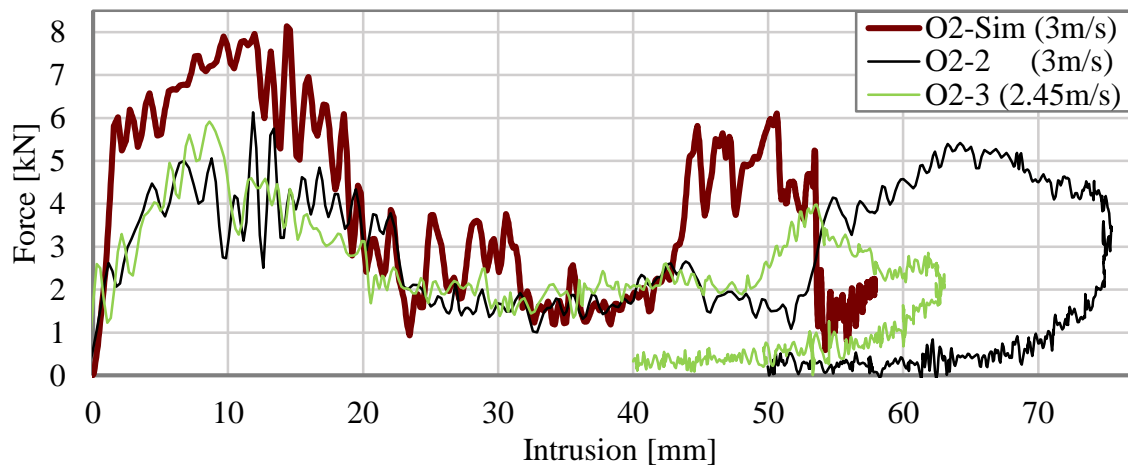


Figure 14: Force curves of the options 2 (O2)

5 CONCLUSIONS

This paper presents the adaptations that are necessary to consider composites during the optimization with the Graph and Heuristic Based Topology Optimization in a crashworthiness application. First, flange connections were introduced that allow to split the structure in several parts and enable to manufacture the structures by vacuum infusion without undercuts. Then a new heuristic was presented, that detects areas with sudden element failure and supports these locations with perpendicular walls. Also new options for composite specific design variables were presented. To demonstrate the process, the method was applied for a composite profile that is laterally impacted by a drop weight. During an optimization the maximum occurring force was minimized by up to 41% while not exceeding the maximum allowed intrusion. Since an optimization with discrete specified composite layups is not implemented yet, the layups of three chosen optimization designs were adjusted to fit the available composite stacks. The comparison between the drop tests and the simulations shows great deviations in the mechanical behavior. Especially the modeling of the adhesive does not depict the real behavior and underlines the importance of material testing. In addition the manufacturing by hand certainly favoured differing results. The start designs deformed more stable, but were not able to utilize the full potential of the allowed deformation space. In contrast the tests of the optimized designs exceed the intrusion restriction and show an undesired deformation behavior with risk of losing the structural integrity, which is caused by the more complex structures and the failing flanges. None of the structures experienced crushing during the tests, which is an important mechanism to increase the specific energy absorption of the composite. New heuristics could try to favour this mode of failure, although walls in lateral impacts rather tend to bending and breaking.

The method will be enhanced in further projects to fully capture the optimization of composite structures. Working with heuristics that analyze simulation data and suggest producible designs is a great opportunity for the optimization of crashworthiness applications in the future, where currently most structures are designed by empirical knowledge or trial and error without maxing out the potential of the structures.

REFERENCES

- [1] C. Ortmann and A. Schumacher, Graph and heuristic based topology optimization of crash loaded structures, *Structural and Multidisciplinary Optimization*, 47 (6), 839-854, 2013.
- [2] M. P. Bendsøe and O. Sigmund, *Topology Optimization*, Springer-Verlag, Berlin Heidelberg, 2004.
- [3] A. Schumacher, *Optimierung mechanischer Strukturen*, Springer-Verlag, Berlin Heidelberg, 2013.
- [4] J. Fang, G. Sun, N. Qiu et al., On design optimization for structural crashworthiness and its state of the art, *Structural and Multidisciplinary Optimization*, 55 (3), 1091-1119, 2017.
- [5] D. Schneider, A. Schumacher, Finding best layouts for rips on surfaces for crash loads using the Graph and Heuristic Based Topology Optimization, *Advances in Structural and Multidisciplinary Optimization, Proceedings of the 12th World Congress of Structural and Multidisciplinary Optimization (WCSMO12)* Springer Nature, 1615-1628, 2018